

Low-Rank Graph Contrastive Learning for Node Classification

Anonymous authors

Paper under double-blind review

Abstract

Graph Neural Networks (GNNs) have been widely used to learn node representations and with outstanding performance on various tasks such as node classification. However, noise, which inevitably exists in real-world graph data, would considerably degrade the performance of GNNs revealed by recent studies. In this work, we propose a novel and robust GNN encoder, Low-Rank Graph Contrastive Learning (LR-GCL). Our method performs transductive node classification in two steps. First, a low-rank GCL encoder named LR-GCL is trained by prototypical contrastive learning with low-rank regularization. Next, using the features produced by LR-GCL, a linear transductive classification algorithm is used to classify the unlabeled nodes in the graph. Our LR-GCL is inspired by the low frequency property of the graph data and its labels, and it is also theoretically motivated by our sharp generalization bound for transductive learning. To the best of our knowledge, our theoretical result is among the first to theoretically demonstrate the advantage of low-rank learning in graph contrastive learning supported by strong empirical performance. Extensive experiments on public benchmarks demonstrate the superior performance of LR-GCL and the robustness of the learned node representations. The code of LR-GCL is available at <https://anonymous.4open.science/r/LRGCL/>.

1 Introduction

Graph Neural Networks (GNNs) have become popular tools for node representation learning in recent years (Kipf & Welling, 2017; Bruna et al., 2014; Hamilton et al., 2017; Xu et al., 2019). Most prevailing GNNs (Kipf & Welling, 2017; Zhu & Koniusz, 2020) leverage the graph structure and obtain the representation of nodes in a graph by utilizing the features of their connected nodes. Benefiting from such propagation mechanism, node representations obtained by GNN encoders have demonstrated superior performance on various downstream tasks such as semi-supervised node classification and node clustering.

Although GNNs have achieved great success in node representation learning, many existing GNN approaches do not consider the noise in the input graph. In fact, noise inherently exists in the graph data for many real-world applications. Such noise may be present in node attributes or node labels, which forms two types of noise, attribute noise and label noise. Recent works, such as (Patrini et al., 2017), have evidenced that noisy inputs hurt the generalization capability of neural networks. Moreover, noise in a subset of the graph data can easily propagate through the graph topology to corrupt the remaining nodes in the graph data. Nodes that are corrupted by noise or falsely labeled would adversely affect the representation learning of themselves and their neighbors.

While manual data cleaning and labeling could be remedies to the consequence of noise, they are expensive processes and difficult to scale, thus not able to handle almost infinite amount of noisy data online. Therefore, it is crucial to design a robust GNN encoder that could make use of noisy training data while circumventing the adverse effect of noise. In this paper, we propose a novel GCL encoder termed Low-Rank Graph Contrastive Learning (LR-GCL) to improve the robustness and the generalization capabilities of node representations for GNNs.

1.1 Contributions

Our contributions are as follows.

First, we present a novel and provable GCL encoder termed Low-Rank Graph Contrastive Learning (LR-GCL). Our algorithm is inspired by the low frequency property illustrated in Figure 1. That is, the low-rank projection of the ground truth clean labels possesses the majority of the information of the clean labels, and projection of the label noise is mostly uniform over all the eigenvectors of a kernel matrix used in classification. Inspired by this observation, LR-GCL adds the truncated nuclear norm as a low-rank regularization term in the loss function of the regular prototypical graph contrastive learning. As a result, the features produced by LR-GCL tend to be low-rank, and such low-rank features are the input to the linear transductive classification algorithm. We provide a novel generalization bound for the test loss on the unlabeled data, and our bound is among the first few works which exhibit the advantage of learning with low-rank features for transductive classification with the presence of noise.

Second, we provide strong theoretical guarantee on the generalization capability of the linear transductive algorithm with the low-rank features produced by LR-GCL as the input. Extensive experimental results on popular graph datasets evidence the advantage of LR-GCL over competing methods for node classification on noisy graph data.

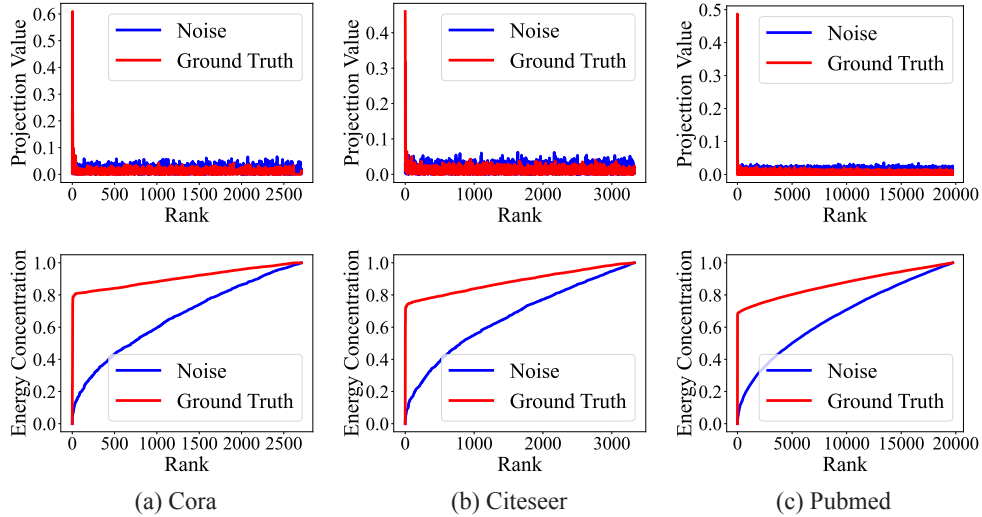


Figure 1: Eigen-projection (first row) and signal concentration ratio (second row) on Cora, Citeseer, and Pubmed. To compute the eigen-projection, we first calculate the eigenvectors \mathbf{U} of the feature gram matrix $\mathbf{K} = \mathbf{H}\mathbf{H}^\top$, then the eigen-projection value is computed by $\mathbf{p} = \frac{1}{C} \sum_{c=1}^C \frac{\|\mathbf{U}^\top \tilde{\mathbf{Y}}^{(c)}\|_2^2}{\|\tilde{\mathbf{Y}}^{(c)}\|_2^2} \in \mathbb{R}^N$, where C is the number of classes, and $\tilde{\mathbf{Y}} \in \{0,1\}^{N \times C}$ is the one-hot clean labels of all the nodes, $\tilde{\mathbf{Y}}^{(c)}$ is the c -th column of $\tilde{\mathbf{Y}}$. With the presence of label noise $\mathbf{N} \in \mathbb{R}^{N \times C}$, the observed label matrix is $\mathbf{Y} = \tilde{\mathbf{Y}} + \mathbf{N}$. The eigen-projection \mathbf{p}_r for $r \in [N]$ reflects the amount of the signal projected onto the r -th eigenvector of \mathbf{K} , and the signal concentration ratio of a rank r reflects the proportion of signal projected onto the top r eigenvectors of \mathbf{K} . The signal concentration ratio for rank r is computed by $\|\mathbf{p}^{(1:r)}\|_2$, where $\mathbf{p}^{(1:r)}$ contains the first r elements of \mathbf{p} . It is observed from the red curves in the first row that the projection of the ground truth clean labels mostly concentrates on the top eigenvectors of \mathbf{K} . On the other hand, the projection of label noise, computed by $\frac{1}{C} \sum_{c=1}^C \frac{\|\mathbf{U}^\top \mathbf{N}^{(c)}\|_2^2}{\|\mathbf{N}^{(c)}\|_2^2} \in \mathbb{R}^N$, is relatively uniform over all the eigenvectors, as illustrated by the blue curves in the first row. For example, by the rank $r = 0.2 \min\{N, d\}$, the signal concentration ratio of $\tilde{\mathbf{Y}}$ for Cora, Citeseer, and Pubmed are 0.844, 0.809, and 0.784 respectively. We refer to such property as the **low frequency property**, which suggests that we can learn a low-rank portion of the observed label \mathbf{Y} which covers most information in the ground truth clean label while only learning a small portion of the label noise. Figure 3 in the appendix further illustrates the low frequency property on more datasets.

2 Related Works

2.1 Graph Neural Networks

Graph neural networks (GNNs) have recently become popular tools for node representation learning. Given the difference in the convolution domain, current GNNs fall into two classes. The first class features spectral convolution (Bruna et al., 2014; Kipf & Welling, 2017), and the second class (Hamilton et al., 2017; Velićković et al., 2017; Xu et al., 2019) generates node representations by sampling and propagating features from their neighborhood. To learn node representation without node labels, contrastive learning has recently been applied to the training of GNNs (Suresh et al., 2021; Thakoor et al., 2021; Wang et al., 2022; Lee et al., 2022; Feng et al., 2022a; Zhang et al., 2023; Lin et al., 2023). Most proposed graph contrastive learning methods (Velićković et al., 2019; Sun et al., 2019; Hu et al., 2019; Jiao et al., 2020; Peng et al., 2020; You et al., 2021; Jin et al., 2021; Mo et al., 2022) create multiple views of the unlabeled input graph and maximize agreement between the node representations of these views. For example, SFA (Zhang et al., 2023) manipulates the spectrum of the node embeddings to construct augmented views in graph contrastive learning. In addition to constructing node-wise augmented views, recent works (Xu et al., 2021; Guo et al., 2022; Li et al., 2021) propose to perform contrastive learning between node representations and semantic prototype representations (Snell et al., 2017; Arik & Pfister, 2020; Allen et al., 2019; Xu et al., 2020) to encode the global semantics information.

However, as pointed out by (Dai et al., 2021), the performance of GNNs can be easily degraded by noisy training data (NT et al., 2019). Moreover, the adverse effects of noise in a subset of nodes can be exaggerated by being propagated to the remaining nodes through the network structure, exacerbating the negative impact of noise. Unlike previous GCL methods, we propose using contrastive learning to train GNN encoders that are robust to noise existing in the labels and attributes of nodes.

2.2 Existing Methods Handling Noisy Data

Previous works (Zhang et al., 2021) have shown that deep neural networks usually generalize badly when trained on input with noise. Existing literature on robust learning mostly fall into two categories. The first category (Patrini et al., 2017; Goldberger & Ben-Reuven, 2016) mitigates the effects of noisy inputs by correcting the computation of loss function, known as loss corruption. The second category aims to select clean samples from noisy inputs for the training (Malach & Shalev-Shwartz, 2017; Jiang et al., 2018; Yu et al., 2019; Li et al., 2020; Han et al., 2018), known as sample selection.

To improve the performance of GNNs on graph data with noise, NRGNN (Dai et al., 2021) first introduces a graph edge predictor to predict missing links for connecting unlabeled nodes with labeled nodes. RTGNN (Qian et al., 2022) trains a robust GNN classifier with scarce and noisy node labels. It first classifies labeled nodes into clean and noisy ones and adopts reinforcement supervision to correct noisy labels. To improve the robustness of the node classifier on the dynamic graph, GraphSS (Zhuang & Al Hasan, 2022) proposes to generalize noisy supervision as a kind of self-supervised learning method, which regards the noisy labels, including both manual-annotated labels and auto-generated labels, as one kind of self-information for each node. Different from previous works, we aim to improve the robustness of GNN encoders for node classification by applying low-rank regularization during the training of the transductive classifier.

3 Problem Setup

3.1 Notations

An attributed graph with N nodes is denoted as $\mathcal{G} = (\mathcal{V}, \mathcal{E}, \mathbf{X})$, where the node set $\mathcal{V} = \{v_1, v_2, \dots, v_N\}$ and the edge set $\mathcal{E} \subseteq \mathcal{V} \times \mathcal{V}$ represent the nodes and edges of the graph, respectively. The matrix $\mathbf{X} \in \mathbb{R}^{N \times D}$ denotes the attributes for all the nodes, where D is the dimension of node attributes. The adjacency matrix $\mathbf{A} \in \{0, 1\}^{N \times N}$ for \mathcal{G} has elements $\mathbf{A}_{ij} = 1$ if there is an edge $(v_i, v_j) \in \mathcal{E}$. When self-loops are added to the graph, the modified adjacency matrix is given by $\tilde{\mathbf{A}} = \mathbf{A} + \mathbf{I}$, and $\tilde{\mathbf{D}}$ is the diagonal degree matrix corresponding to $\tilde{\mathbf{A}}$. The notation $[N]$ denotes all natural numbers from 1 to N inclusive. \mathcal{L} is a subset of

$[N]$ of size m , and $\mathcal{U} = [N] \setminus \mathcal{L}$ and $|\mathcal{U}| = u$. Let $\mathcal{V}_{\mathcal{L}}$ and $\mathcal{V}_{\mathcal{U}}$ denote the set of labeled nodes and unlabeled test nodes, respectively, and $|\mathcal{V}_{\mathcal{L}}| = m$, $|\mathcal{V}_{\mathcal{U}}| = u$. Let $\mathbf{u} \in \mathbb{R}^N$ be a vector, we use $[\mathbf{u}]_{\mathcal{A}}$ to denote a vector formed by elements of \mathbf{u} with indices in \mathcal{A} for $\mathcal{A} \subseteq [N]$. If \mathbf{u} is a matrix, then $[\mathbf{u}]_{\mathcal{A}}$ denotes a submatrix formed by rows of \mathbf{u} with row indices in \mathcal{A} . $\|\cdot\|_{\text{F}}$ denotes the Frobenius norm of a matrix, and $\|\cdot\|_p$ denotes the p -norm of a vector.

3.2 Graph Convolution Network (GCN)

To learn the node representation from the attributes \mathbf{X} and the graph structure \mathbf{A} , one simple yet effective neural network model is Graph Convolution Network (GCN). GCN is originally proposed for semi-supervised node classification, which consists of two graph convolution layers. In our work, we use GCN as the backbone of the proposed LR-GCL, which is the GCL encoder, to obtain node representation $\mathbf{H} \in \mathbb{R}^{N \times d}$, where the i -th row of \mathbf{H} is the node representation of v_i . In this manner, the output of LR-GCL is $\mathbf{H} = g(\mathbf{X}, \mathbf{A}) = \sigma(\hat{\mathbf{A}}\sigma(\hat{\mathbf{A}}\mathbf{X}\tilde{\mathbf{W}}^{(0)})\tilde{\mathbf{W}}^{(1)})$, where $\hat{\mathbf{A}} = \tilde{\mathbf{D}}^{-1/2}\tilde{\mathbf{A}}\tilde{\mathbf{D}}^{-1/2}$, $\tilde{\mathbf{W}}^{(0)}$ and $\tilde{\mathbf{W}}^{(1)}$ are the weight matrices, and σ is the activation function ReLU. The robust and low-rank node representations produced by the LR-GCL are used to perform transductive node classification by a linear classifier. LR-GCL and the linear transductive node classification algorithm are detailed in Section 4.

3.3 Problem Description

Noise usually exists in the input node attributes or labels of real-world graphs, which degrades the quality of the node representation obtained by common GCL encoders and affects the performance of the classifier trained on such representations. We aim to obtain node representations robust to noise in two cases, where noise is present in either the labels of $\mathcal{V}_{\mathcal{L}}$ or in the input node attributes \mathbf{X} . That is, we consider either noisy label or noisy input node attributes.

The goal of LR-GCL is to learn low-rank node representations by $\mathbf{H} = g(\mathbf{X}, \mathbf{A})$ such that the node representations $\{\mathbf{h}_i\}_{i=1}^N$ are robust to noise in the above two cases, where $g(\cdot)$ is the LR-GCL encoder. In our work, g is a two-layer GCN introduced in Section 3.2. The low-rank node representations by LR-GCL, $\mathbf{H} = \{\mathbf{h}_1; \mathbf{h}_2; \dots; \mathbf{h}_N\} \in \mathbb{R}^{N \times d}$, are used for transductive node classification by a linear classifier. In transductive node classification, a linear transductive classifier is trained on $\mathcal{V}_{\mathcal{L}}$, and then the classifier predicts the labels of the unlabeled test nodes in $\mathcal{V}_{\mathcal{U}}$.

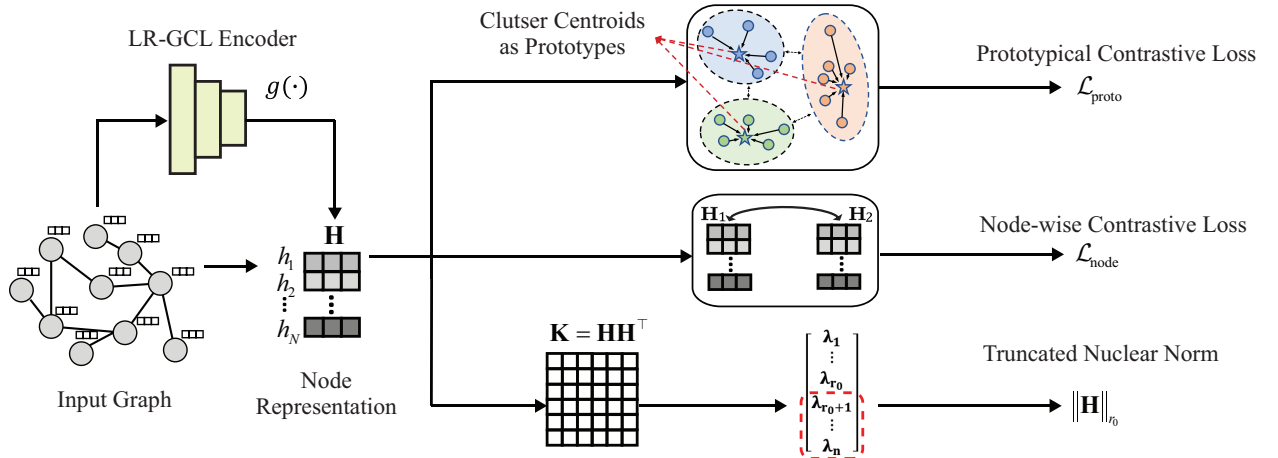


Figure 2: Illustration of the LR-GCL framework.

4 Methods

4.1 Low-Rank GCL: Low-Rank Graph Contrastive Learning

Preliminary of Prototypical GCL. The general node representation learning aims to train an encoder $g(\cdot)$, which is a two-layer Graph Convolution Neural Network (GCN) (Kipf & Welling, 2017), to generate discriminative node representations. In our work, we adopt contrastive learning to train the GCL encoder $g(\cdot)$. To perform contrastive learning, two different views, $G^1 = (\mathbf{X}^1, \mathbf{A}^1)$ and $G^2 = (\mathbf{X}^2, \mathbf{A}^2)$, are generated by node dropping, edge perturbation, and attribute masking. The representation of two generated views are denoted as $\mathbf{H}^1 = g(\mathbf{X}^1, \mathbf{A}^1)$ and $\mathbf{H}^2 = g(\mathbf{X}^2, \mathbf{A}^2)$, with \mathbf{H}_i^1 and \mathbf{H}_i^2 being the i -th row of \mathbf{H}^1 and \mathbf{H}^2 , respectively. It is preferred that the mutual information between \mathbf{H}^1 and \mathbf{H}^2 is maximized. For computational reason, its lower bound is usually used as the objective for contrastive learning. We use InfoNCE (Li et al., 2021) as our node-wise contrastive loss. In addition to the node-wise contrastive learning, we also adopt prototypical contrastive learning (Li et al., 2021) to capture semantic information in the node representations, which is interpreted as maximizing the mutual information between node representation and a set of estimated cluster prototypes $\{\mathbf{c}_1, \dots, \mathbf{c}_K\}$. Following (Li et al., 2021; Snell et al., 2017), we use K -means to cluster the node representations $\{\mathbf{h}_i\}_{i=1}^n$ into K clusters and take the clustering centroid of the k -th cluster as the k -th prototype $\mathbf{c}_k = \frac{1}{|S_k|} \sum_{\mathbf{h}_i \in S_k} \mathbf{h}_i$ for all $k \in [K]$. The loss function of Prototypical GCL is comprised of two terms, \mathcal{L}_{node} , the loss function for node-wise contrastive learning, and \mathcal{L}_{proto} , the prototypical contrastive learning loss, which are presented below:

$$\mathcal{L}_{node} = -\frac{1}{N} \sum_{i=1}^N \log \frac{s(\mathbf{H}_i^1, \mathbf{H}_i^2)}{s(\mathbf{H}_i^1, \mathbf{H}_i^2) + \sum_{j=1}^N s(\mathbf{H}_i^1, \mathbf{H}_j^2)}, \quad \mathcal{L}_{proto} = -\frac{1}{N} \sum_{i=1}^N \log \frac{\exp(\mathbf{H}_i \cdot \mathbf{c}_k / \tau)}{\sum_{k=1}^K \exp(\mathbf{H}_i \cdot \mathbf{c}_k / \tau)}. \quad (1)$$

Here $s(\mathbf{H}_i^1, \mathbf{H}_i^2)$ is the cosine similarity between two node representations, \mathbf{H}_i^1 and \mathbf{H}_i^2 .

LR-GCL: Low-Rank Graph Contrastive Learning. LR-GCL aims to improve the robustness and generalization capability of the node representations of Prototypical GCL by enforcing the learned feature kernel to be low-rank. The gram matrix \mathbf{K} of the node representations $\mathbf{H} \in \mathbb{R}^{N \times d}$ is calculated by $\mathbf{K} = \mathbf{H}^\top \mathbf{H} \in \mathbb{R}^{N \times N}$. Let $\{\hat{\lambda}_i\}_{i=1}^n$ with $\hat{\lambda}_1 \geq \hat{\lambda}_2 \geq \dots \geq \hat{\lambda}_{\min\{N, d\}} \geq \hat{\lambda}_{\min\{N, d\}+1} = \dots = 0$ be the eigenvalues of \mathbf{K} . In order to encourage the features \mathbf{H} or the gram matrix $\mathbf{H}^\top \mathbf{H}$ to be low-rank, we explicitly add the truncated nuclear norm $\|\mathbf{H}\|_{r_0+1} := \sum_{r=r_0}^n \hat{\lambda}_i$ to the loss function of prototypical GCL. The starting rank $r_0 < \min(n, d)$ is the rank of the features \mathbf{H} we aim to obtain with the LR-GCL encoder, that is, if $\|\mathbf{H}\|_{r_0} = 0$, then $\text{rank}(\mathbf{H}) = r_0$. Therefore, the overall loss function of LR-GCL is

$$\mathcal{L}_{\text{LR-GCL}} = \mathcal{L}_{node} + \mathcal{L}_{proto} + \tau \|\mathbf{H}\|_{r_0}, \quad (2)$$

where $\tau > 0$ is the weighting parameter for the truncated nuclear norm $\|\mathbf{H}\|_{r_0}$. We summarize the training algorithm for the LR-GCL encoder in Algorithm 1. After finishing the training, we calculate the low-rank node feature by $\mathbf{H} = g(\mathbf{A}, \mathbf{X})$.

Motivation of Learning Low-Rank Features. Let $\tilde{\mathbf{Y}} \in \mathbb{R}^{N \times C}$ be the ground truth clean label matrix without noise. By the low frequency property illustrated in Figure 1, the projection of $\tilde{\mathbf{Y}}$ on the top r eigenvectors of \mathbf{K} with a small rank r , such as $r = 0.2N$, covers the majority of the information in $\tilde{\mathbf{Y}}$. On the other hand, the projection of the label noise \mathbf{N} are distributed mostly uniform across all the eigenvectors. This observation motivates low-rank features \mathbf{H} or equivalently, the low-rank gram matrix \mathbf{K} . This is because the low-rank part of the feature matrix \mathbf{H} or the gram matrix \mathbf{K} covers the dominant information in the ground truth label $\tilde{\mathbf{Y}}$ while learning only a small portion of the label noise. Moreover, we remark that the regularization term $\|\mathbf{H}\|_{r_0}$ in the loss function (2) of LR-GCL is also theoretically motivated by the sharp upper bound for the test loss using a linear transductive classifier, presented as (4) in Theorem 4.1. A smaller $\|\mathbf{H}\|_{r_0}$ renders a smaller upper bound for the test loss, which ensures better generalization capability of the linear transductive classifier to be introduced in the next subsection.

4.2 Transductive Node Classification

In this section, we introduce a simple yet standard linear transductive node classification algorithm using the low-rank node representations $\mathbf{H} \in \mathbb{R}^{N \times d}$ produced by the LR-GCL encoder. We present strong theoretical

Algorithm 1 Low-Rank Graph Contrastive Learning (LR-GCL)**Input:** The input attribute matrix \mathbf{X} , adjacency matrix \mathbf{A} , and the training epochs t_{\max} .**Output:** The parameters of LR-GCL encoder g

- 1: Initialize the parameter of LR-GCL encoder g
- 2: **for** $t \leftarrow 1$ to t_{\max} **do**
- 3: Calculate node representations by $\mathbf{H} = g(\mathbf{X}, \mathbf{A})$, generate augmented views G^1, G^2 , and calculate node representations $\mathbf{H}^1 = g(\mathbf{X}^1, \mathbf{A}^1)$ and $\mathbf{H}^2 = g(\mathbf{X}^2, \mathbf{A}^2)$
- 4: Cluster node representations $\{\mathbf{h}_i\}_{i=1}^n$ into K clusters $\{S_k\}_{k=1}^K$ with K -means clustering
- 5: Update the prototype \mathbf{c}_k as the centroid of S_k by $\mathbf{c}_k = \frac{1}{|S_k|} \sum_{\mathbf{h}_i \in S_k} \mathbf{h}_i$ for all $k \in [K]$
- 6: Calculate the eigenvalues $\{\lambda_i\}_{i=1}^N$ of the feature kernel $\mathbf{H}^\top \mathbf{H}$
- 7: Update the parameters of LR-GCL encoder g by one step of gradient descent on the loss \mathcal{L}_{rep}
- 8: **end for**
- 9: **return** The LR-GCL encoder g

result on the generalization bound for the test loss for our low-rank transductive algorithm with the presence of label noise.

We first give basic notations for our algorithm. Let $\mathbf{y}_i \in \mathbb{R}^C$ be the observed one-hot class label vector for node v_i for all $i \in [N]$, and define $\mathbf{Y} := [\mathbf{y}_1; \mathbf{y}_2; \dots; \mathbf{y}_N] \in \mathbb{R}^{N \times C}$ be the observed label matrix which may contain label noise $\mathbf{N} \in \mathbb{R}^{N \times C}$. We define $\mathbf{F}(\mathbf{W}) = \mathbf{H}\mathbf{W}$ as the linear output of the transductive classifier with $\mathbf{W} \in \mathbb{R}^{d \times C}$ being the weight matrix for the classifier. Our transductive classifier uses $\text{softmax}(\mathbf{F}(\mathbf{W})) \in \mathbb{R}^{N \times C}$ for prediction of the labels of the test nodes. We train the transductive classifier by minimizing the regular cross-entropy on the labeled nodes through

$$\min_{\mathbf{W}} L(\mathbf{W}) = \frac{1}{m} \sum_{v_i \in \mathcal{V}_{\mathcal{L}}} \text{KL}(\mathbf{y}_i, [\text{softmax}(\mathbf{H}\mathbf{W})]_i), \quad (3)$$

where KL is the KL divergence between the label \mathbf{y}_i and the softmax of the classifier output at node v_i . We use a regular gradient descent to optimize (3) with a learning rate $\eta \in (0, \frac{1}{\lambda_1})$. \mathbf{W} is initialized by $\mathbf{W}^{(0)} = \mathbf{0}$, and at the t -th iteration of gradient descent for $t \geq 1$, \mathbf{W} is updated by $\mathbf{W}^{(t)} = \mathbf{W}^{(t-1)} - \eta \nabla_{\mathbf{W}} L(\mathbf{W})|_{\mathbf{W}=\mathbf{W}^{(t-1)}}$.

Define $\mathbf{F}(\mathbf{W}, t) := \mathbf{H}\mathbf{W}^{(t)}$ as the output of the classifier after the t -th iteration of gradient descent for $t \geq 1$. We have the following theoretical result, Theorem 4.1, on the Mean Squared Error (MSE) loss of the unlabeled test nodes $\mathcal{V}_{\mathcal{U}}$ measured by the gap between $[\mathbf{F}(\mathbf{W}, t)]_{\mathcal{U}}$ and $[\mathbf{Y}]_{\mathcal{U}}$ when using the low-rank feature \mathbf{H} with $r_0 \in [n]$, which is the generalization error bound for the linear transductive classifier using $\mathbf{F}(\mathbf{W}) = \mathbf{H}\mathbf{W}$ to predict the labels of the unlabeled nodes. Similar to existing works (Kothapalli et al., 2023) that uses the Mean Squared Error (MSE) to analyze the optimization and the generalization of GNNs, we employ the MSE loss to provide the generalization error of the node classifier in the following theorem. It is remarked that the MSE loss is necessary for the generalization analysis of transductive learning using transductive local Rademacher complexity (Tolstikhin et al., 2014; Yang, 2023).

Theorem 4.1. Let $m \geq cN$ for a constant $c \in (0, 1)$, and $r_0 \in [n]$. Assume that a set \mathcal{L} with $|\mathcal{L}| = m$ is sampled uniformly without replacement from $[N]$, and the remaining nodes $\mathcal{V}_{\mathcal{U}} = \mathcal{V} \setminus \mathcal{V}_{\mathcal{L}}$ are the test nodes. Then for every $x > 0$, with probability at least $1 - \exp(-x)$, after the t -th iteration of gradient descent for all $t \geq 1$, we have

$$\begin{aligned} \mathcal{U}_{\text{test}}(t) &:= \frac{1}{u} \|\mathbf{F}(\mathbf{W}, t) - \mathbf{Y}\|_{\mathcal{U}}^2 \\ &\leq \frac{c_0}{m} \left\| \left(\mathbf{I}_m - \eta [\mathbf{K}]_{\mathcal{L}, \mathcal{L}} \right)^t [\mathbf{Y}]_{\mathcal{L}} \right\|_{\mathcal{F}}^2 + c_1 r_0 \left(\frac{1}{u} + \frac{1}{m} \right) + \|\mathbf{H}\|_{r_0} \left(\frac{1}{\sqrt{u}} + \frac{1}{\sqrt{m}} \right) + \frac{c_2 x}{u}, \end{aligned} \quad (4)$$

where c_0, c_1, c_2 are positive numbers depending on \mathbf{U} , $\{\hat{\lambda}_i\}_{i=1}^{r_0}$, and τ_0 with $\tau_0^2 = \max_{i \in [N]} \mathbf{K}_{ii}$.

This theorem is proved in Section A of the appendix. It is noted that $\mathcal{U}_{\text{test}}(t)$ is the test loss of the unlabeled nodes measured by the distance between the classifier output $\mathbf{F}(\mathbf{W}, t)$ and \mathbf{Y} . We remark that the truncated

nuclear norm $\|\mathbf{H}\|_{r_0}$ appears on the RHS of the upper bound (4), theoretically justifying why we learn the low-rank features \mathbf{H} of the LR-GCL by adding the truncated nuclear norm $\|\mathbf{H}\|_{r_0}$ to the loss of our LR-GCL in (2). Moreover, when the low frequency property holds, which is always the case as demonstrated by Figure 1 and Figure 3 in the appendix, $\left\| \left(\mathbf{I}_m - \eta [\mathbf{K}]_{\mathcal{L}, \mathcal{L}} \right)^t [\mathbf{Y}]_{\mathcal{L}} \right\|_{\mathbf{F}}^2$ would be very small with enough iteration number t .

In our empirical study in the next section, we search for the rank r_0 for the truncated nuclear norm by standard cross-validation for all the graph data sets. In Table 1 of our experimental results, it is observed that the best rank r_0 is always between $0.1 \min \{N, d\}$ and $0.3 \min \{N, d\}$. The overall framework of LR-GCL is illustrated in Figure 2.

5 Experiments

In this section, we evaluate the performance of LR-GCL on public graph datasets. In Section 5.1, we discuss the experimental settings and implementation details of LRA-GCL. The detailed statistics of the benchmark datasets are presented in Section 5.2. In Section 5.3, we present evaluation results of LR-GCL for semi-supervised node classification with different types of noise. In Section 5.4, we compare LR-GCL with existing GCL methods equipped with different types of classifiers. In Section 5.5, we study the kernel complexity of node representations learned by LR-GCL. In Section 5.6, we perform an ablation study on the rank r_0 in the truncated nuclear norm. In Section B.1, we compare the training time of LR-GCL with other baseline methods. Additional eigen-projection and energy concentration ratio results are presented in Section C of the appendix.

Table 1: Selected rank ratio γ and truncated nuclear loss’s weight λ for each dataset.

Hyper-parameters	Cora	Citeseer	PubMed	Coauthor CS	ogbn-arxiv	Wiki-CS	Amazon-Computers	Amazon-Photos
τ	0.10	0.10	0.10	0.20	0.10	0.25	0.20	0.20
γ	0.2	0.2	0.3	0.3	0.4	0.2	0.2	0.3

5.1 Experimental Settings

In our experiment, we adopt eight widely used graph benchmark datasets, namely Cora, Citeseer, PubMed (Sen et al., 2008), Coauthor CS, ogbn-arxiv (Hu et al., 2020), Wiki-CS (Mernyei & Cangea, 2020), Amazon-Computers, and Amazon-Photos (Shchur et al., 2018) for the evaluation in node classification. Due to the fact that all public benchmark graph datasets do not come with corrupted labels or attribute noise, we manually inject noise into public datasets to evaluate our algorithm. We follow the commonly used label noise generation methods from the existing work (Han et al., 2020; Dai et al., 2022; Qian et al., 2022) to inject label noise. We generate noisy labels over all classes in two types: (1) Symmetric, where nodes from each class is flipped to other classes with a uniform random probability; (2) Asymmetric, where mislabeling only occurs between similar classes. The percentage of nodes with flipped labels is defined as the label noise level in our experiments. To evaluate the performance of our method with attribute noise, we randomly shuffle a certain percentage of input attributes for each node following (Ding et al., 2022). The percentage of shuffled attributes is defined as the attribute noise level in our experiments.

Table 2: The statistics of the datasets.

Dataset	Nodes	Edges	Features	Classes
Cora	2,708	5,429	1,433	7
CiteSeer	3,327	4,732	3,703	6
PubMed	19,717	44,338	500	3
Coauthor CS	18,333	81,894	6,805	15
ogbn-arxiv	169,343	1,166,243	128	40
Wiki-CS	11,701	215,863	300	10
Amazon-Computers	13,752	245,861	767	10
Amazon-Photos	7,650	119,081	745	8

Tuning r_0, τ by Cross-Validation. We tune the rank r_0 and the weight for the truncated nuclear loss τ by standard cross-validation on each dataset. Let $r_0 = \lceil \gamma \min \{N, d\} \rceil$ where γ is the rank ratio. We

select the values of γ and τ by performing 5-fold cross-validation on 20% of the training data in each dataset. The value of γ is selected from $\{0.1, 0.2, 0.3, 0.4, 0.5, 0.6, 0.7, 0.8, 0.9\}$. The value of τ is selected from $\{0.05, 0.1, 0.15, 0.2, 0.25, 0.3, 0.35, 0.4, 0.45, 0.5\}$. The selected values on each dataset are shown in Table 1.

5.2 Datasets

We evaluate our method on eight public benchmarks that are widely used for node representation learning, namely Cora, Citeseer, PubMed (Sen et al., 2008), Coauthor CS, ogbn-arxiv (Hu et al., 2020), Wiki-CS (Mernyei & Cangea, 2020), Amazon-Computers, and Amazon-Photos (Shchur et al., 2018). Cora, Citeseer, and PubMed are the three most widely used citation networks. Coauthor CS is a co-authorship graph. The ogbn-arxiv is a directed citation graph. Wiki-CS is a hyperlink networks of computer science articles. Amazon-Computers and Amazon-Photos are co-purchase networks of products selling on Amazon.com. We summarize the statistics of all the datasets in Table 2. For all our experiments, we follow the default separation (Shchur et al., 2018; Mernyei & Cangea, 2020; Hu et al., 2020) of training, validation, and test sets on each benchmark.

5.3 Node Classification

Compared Methods. We compare LR-GCL against semi-supervised node representation learning methods, GCN (Kipf & Welling, 2017), GCE (Zhang & Sabuncu, 2018), S²GC (Zhu & Koniusz, 2020), and GRAND+ (Feng et al., 2022b). Furthermore, we include two baseline methods for node classification with label noise, which are NRGNN (Dai et al., 2021) and RTGNN (Qian et al., 2022). We also compare LR-GCL against state-of-the-art GCL methods, including GraphCL (You et al., 2020), MERIT (Jin et al., 2021), SUGRL (Mo et al., 2022), and SFA (Zhang et al., 2023). To demonstrate the power of LR-GCL in learning robust node representation, we also compare LR-GCL with two robust contrastive learning baselines, Jo-SRC (Yao et al., 2021) and Sel-CL (Li et al., 2022), which select clean samples for image data. Since their sample selection methods are general and not limited to the image domain, we adopt these two baselines to the graph domain in our experiments as described below.

Jo-SRC utilizes the Jensen-Shannon divergence to identify clean training samples through a general representation space selection strategy. This approach also incorporates a consistency regularization term into the contrastive loss to enhance robustness. In our adaptation, we apply the sample selection and consistency regularization techniques in Jo-SRC to the state-of-the-art GCL method, MERIT. We modify the graph contrastive loss to integrate the regularization term from Jo-SRC and train the GCL encoder exclusively on the clean samples identified by Jo-SRC.

Sel-CL is designed to learn robust pre-trained representations by selectively forming contrastive pairs from confident examples. These confident examples are identified through the alignment of learned representations with propagated labels, assessed using cross-entropy loss. Sel-CL then selects contrastive pairs that exhibit a representation similarity exceeding a dynamically determined threshold. We adopt the confident contrastive pair selection strategy in Sel-CL to select the confident contrastive pairs in the node representation space. The selection strategy is incorporated into the state-of-the-art GCL method, MERIT.

Experimental Results. We first compare LR-GCL against competing methods for semi-supervised or transductive node classification on input with two types of label noise. To show the robustness of LR-GCL against label noise, we perform the experiments on graphs injected with different levels of label noise ranging from 40% to 80% with a step of 20%. We follow the widely used semi-supervised setting (Kipf & Welling, 2017) for node classification. In LR-GCL, we train a transductive classifier for node classification. Previous GCL methods, including MERIT, SUGRL, and SFA, train a linear layer for inductive classification on top of the node representations learned by contrastive learning without using test data in training. Because LR-GCL is a transductive classifier, for fair comparisons, we also train the compared GCL baselines with the same transductive classifier as that for LR-GCL and a two-layer GCN transductive classifier. The results with different types of classifiers are shown in Section 5.4. For all the baselines in our experiments that perform inductive classification when predicting the labels, we report their best results using their original inductive classifier and two types of transductive classifiers: the same transductive classifier as that for LR-GCL and a two-layer GCN transductive classifier.

Table 3: Performance comparison for node classification on Cora, Citeseer, PubMed, and Wiki-CS with asymmetric label noise, symmetric label noise, and attribute noise.

Dataset	Methods	Noise Level									
		0	40			60			80		
		-	Asymmetric	Symmetric	Attribute	Asymmetric	Symmetric	Attribute	Asymmetric	Symmetric	Attribute
Cora	GCN	0.815±0.005	0.547±0.015	0.636±0.007	0.639±0.008	0.405±0.014	0.517±0.010	0.439±0.012	0.265±0.012	0.354±0.014	0.317±0.013
	S ² GC	0.835±0.002	0.569±0.007	0.664±0.007	0.661±0.007	0.422±0.010	0.535±0.010	0.454±0.011	0.279±0.014	0.366±0.014	0.320±0.013
	GCE	0.819±0.004	0.573±0.011	0.652±0.008	0.650±0.014	0.449±0.011	0.509±0.011	0.445±0.015	0.280±0.013	0.353±0.013	0.325±0.015
	UnionNET	0.820±0.006	0.569±0.014	0.664±0.007	0.653±0.012	0.452±0.010	0.541±0.010	0.450±0.009	0.283±0.014	0.370±0.011	0.320±0.012
	NRGNN	0.822±0.006	0.571±0.019	0.676±0.007	0.645±0.012	0.470±0.014	0.548±0.014	0.451±0.011	0.282±0.022	0.373±0.012	0.326±0.010
	RTGNN	0.828±0.003	0.570±0.010	0.682±0.008	0.678±0.011	0.474±0.011	0.555±0.010	0.457±0.009	0.280±0.011	0.386±0.014	0.342±0.016
	SUGRL	0.834±0.005	0.564±0.011	0.674±0.012	0.675±0.009	0.468±0.011	0.552±0.011	0.452±0.012	0.280±0.012	0.381±0.012	0.338±0.014
	MERIT	0.831±0.005	0.560±0.008	0.670±0.008	0.671±0.009	0.467±0.013	0.547±0.013	0.450±0.014	0.277±0.013	0.385±0.013	0.335±0.009
	ARIEL	0.843±0.004	0.573±0.013	0.681±0.010	0.675±0.009	0.471±0.012	0.553±0.012	0.455±0.014	0.284±0.014	0.389±0.013	0.343±0.013
	SFA	0.839±0.010	0.564±0.011	0.677±0.013	0.676±0.015	0.473±0.014	0.549±0.014	0.457±0.014	0.282±0.016	0.389±0.013	0.344±0.017
	Sel-Cl	0.828±0.002	0.570±0.010	0.685±0.012	0.676±0.009	0.472±0.013	0.554±0.014	0.455±0.011	0.282±0.017	0.389±0.013	0.341±0.015
	Jo-SRC	0.825±0.005	0.571±0.006	0.684±0.013	0.679±0.007	0.473±0.011	0.556±0.008	0.458±0.012	0.285±0.013	0.387±0.018	0.345±0.018
	GRAND+	0.858±0.006	0.570±0.009	0.682±0.007	0.678±0.011	0.472±0.010	0.554±0.008	0.456±0.012	0.284±0.015	0.387±0.015	0.345±0.013
	LR-GCL	0.858±0.006	0.589±0.011	0.713±0.007	0.695±0.011	0.492±0.011	0.587±0.013	0.477±0.012	0.306±0.012	0.419±0.012	0.363±0.011
Citeseer	GCN	0.703±0.005	0.475±0.023	0.501±0.013	0.529±0.009	0.351±0.014	0.341±0.014	0.372±0.011	0.291±0.022	0.281±0.019	0.290±0.014
	S ² GC	0.736±0.005	0.488±0.013	0.528±0.013	0.553±0.008	0.363±0.012	0.367±0.014	0.390±0.013	0.304±0.024	0.284±0.019	0.288±0.011
	GCE	0.705±0.004	0.490±0.016	0.512±0.014	0.540±0.014	0.362±0.015	0.352±0.010	0.381±0.009	0.309±0.012	0.285±0.014	0.285±0.011
	UnionNET	0.706±0.006	0.499±0.015	0.547±0.014	0.545±0.013	0.379±0.013	0.399±0.013	0.379±0.012	0.322±0.021	0.302±0.013	0.290±0.012
	NRGNN	0.710±0.006	0.498±0.015	0.546±0.015	0.538±0.011	0.382±0.016	0.412±0.016	0.377±0.012	0.336±0.021	0.309±0.018	0.284±0.009
	RTGNN	0.746±0.008	0.498±0.007	0.556±0.007	0.550±0.012	0.392±0.010	0.424±0.013	0.390±0.014	0.348±0.017	0.308±0.016	0.302±0.011
	SUGRL	0.730±0.005	0.493±0.011	0.541±0.011	0.544±0.010	0.376±0.009	0.421±0.009	0.388±0.009	0.339±0.010	0.305±0.010	0.300±0.009
	MERIT	0.740±0.007	0.496±0.012	0.536±0.012	0.542±0.010	0.383±0.011	0.425±0.011	0.387±0.008	0.344±0.014	0.301±0.014	0.295±0.009
	SFA	0.740±0.011	0.502±0.014	0.532±0.015	0.547±0.013	0.390±0.014	0.433±0.014	0.389±0.012	0.347±0.016	0.312±0.015	0.299±0.013
	ARIEL	0.727±0.007	0.500±0.008	0.550±0.013	0.548±0.008	0.391±0.009	0.427±0.012	0.389±0.014	0.349±0.014	0.307±0.013	0.299±0.013
	Sel-Cl	0.725±0.008	0.499±0.012	0.551±0.010	0.549±0.008	0.389±0.011	0.426±0.008	0.391±0.020	0.350±0.018	0.310±0.015	0.300±0.017
	Jo-SRC	0.730±0.005	0.500±0.013	0.555±0.011	0.551±0.011	0.394±0.013	0.425±0.013	0.393±0.013	0.351±0.013	0.305±0.018	0.303±0.013
	GRAND+	0.756±0.004	0.497±0.010	0.553±0.010	0.552±0.011	0.390±0.013	0.422±0.013	0.387±0.013	0.348±0.013	0.309±0.014	0.302±0.012
	LR-GCL	0.757±0.010	0.520±0.013	0.581±0.013	0.570±0.007	0.410±0.014	0.455±0.014	0.406±0.012	0.369±0.012	0.335±0.014	0.318±0.010
PubMed	GCN	0.790±0.007	0.584±0.022	0.574±0.012	0.595±0.012	0.405±0.025	0.386±0.011	0.488±0.013	0.305±0.022	0.295±0.013	0.423±0.013
	S ² GC	0.802±0.005	0.585±0.023	0.589±0.013	0.610±0.009	0.421±0.030	0.401±0.014	0.497±0.012	0.310±0.039	0.290±0.019	0.431±0.010
	GCE	0.792±0.009	0.589±0.018	0.581±0.011	0.590±0.014	0.430±0.012	0.399±0.012	0.491±0.010	0.311±0.021	0.301±0.011	0.424±0.012
	UnionNET	0.793±0.008	0.603±0.020	0.620±0.012	0.592±0.012	0.445±0.022	0.424±0.013	0.489±0.015	0.313±0.025	0.327±0.015	0.435±0.009
	NRGNN	0.797±0.008	0.602±0.022	0.618±0.013	0.603±0.008	0.443±0.012	0.434±0.012	0.499±0.009	0.330±0.023	0.325±0.013	0.433±0.011
	RTGNN	0.797±0.004	0.610±0.008	0.622±0.010	0.614±0.012	0.455±0.010	0.455±0.011	0.501±0.011	0.335±0.013	0.338±0.017	0.452±0.013
	SUGRL	0.819±0.005	0.603±0.013	0.615±0.013	0.615±0.010	0.445±0.011	0.441±0.011	0.501±0.007	0.321±0.009	0.321±0.009	0.446±0.010
	MERIT	0.801±0.004	0.593±0.011	0.612±0.011	0.613±0.011	0.447±0.012	0.443±0.012	0.497±0.009	0.328±0.011	0.323±0.011	0.445±0.009
	ARIEL	0.800±0.003	0.610±0.013	0.622±0.010	0.615±0.011	0.453±0.012	0.453±0.012	0.502±0.014	0.331±0.014	0.336±0.018	0.457±0.013
	SFA	0.804±0.010	0.596±0.011	0.615±0.011	0.609±0.011	0.447±0.014	0.446±0.017	0.499±0.014	0.330±0.011	0.327±0.011	0.447±0.014
	Sel-Cl	0.799±0.005	0.605±0.014	0.625±0.012	0.614±0.012	0.455±0.014	0.449±0.010	0.502±0.008	0.334±0.021	0.332±0.014	0.456±0.014
	Jo-SRC	0.801±0.005	0.613±0.010	0.624±0.013	0.617±0.013	0.453±0.008	0.455±0.013	0.504±0.013	0.330±0.015	0.334±0.018	0.459±0.018
	GRAND+	0.845±0.006	0.610±0.011	0.624±0.013	0.617±0.013	0.453±0.008	0.453±0.011	0.503±0.010	0.331±0.014	0.337±0.013	0.458±0.014
	LR-GCL	0.845±0.009	0.637±0.014	0.645±0.015	0.637±0.011	0.479±0.011	0.484±0.013	0.526±0.011	0.356±0.011	0.360±0.012	0.482±0.014
Coauthor-CS	GCN	0.918±0.001	0.645±0.009	0.656±0.006	0.702±0.010	0.511±0.013	0.501±0.009	0.531±0.010	0.429±0.022	0.389±0.011	0.415±0.013
	S ² GC	0.918±0.001	0.657±0.012	0.663±0.006	0.713±0.010	0.516±0.013	0.514±0.009	0.556±0.009	0.437±0.020	0.396±0.010	0.422±0.012
	GCE	0.922±0.003	0.662±0.017	0.659±0.007	0.705±0.014	0.515±0.016	0.502±0.007	0.539±0.009	0.443±0.017	0.389±0.012	0.412±0.011
	UnionNET	0.918±0.002	0.669±0.023	0.671±0.013	0.706±0.012	0.525±0.011	0.529±0.011	0.540±0.012	0.458±0.015	0.401±0.011	0.420±0.007
	NRGNN	0.919±0.002	0.678±0.014	0.689±0.009	0.705±0.012	0.545±0.021	0.556±0.011	0.546±0.011	0.461±0.012	0.410±0.012	0.417±0.007
	RTGNN	0.920±0.005	0.678±0.012	0.691±0.009	0.712±0.008	0.559±0.010	0.569±0.011	0.560±0.008	0.455±0.015	0.415±0.015	0.412±0.014
	SUGRL	0.922±0.005	0.675±0.010	0.695±0.010	0.714±0.006	0.550±0.011	0.560±0.011	0.561±0.007	0.449±0.011	0.411±0.011	0.429±0.008
	MERIT	0.924±0.004	0.679±0.011	0.689±0.008	0.709±0.005	0.552±0.014	0.562±0.014	0.562±0.011	0.452±0.013	0.403±0.013	0.426±0.005
	ARIEL	0.925±0.004	0.682±0.011	0.699±0.009	0.712±0.005	0.555±0.011	0.566±0.011	0.556±0.011	0.454±0.014	0.415±0.019	0.427±0.013
	SFA	0.925±0.009	0.682±0.011	0.690±0.012	0.715±0.012	0.555±0.015	0.567±0.014	0.565±0.013	0.458±0.013	0.402±0.013	0.429±0.015
	Sel-Cl	0.922±0.008	0.684±0.009	0.694±0.012	0.714±0.010	0.557±0.013	0.568±0.013	0.566±0.010	0.457±0.013	0.412±0.017	0.425±0.009
	Jo-SRC	0.921±0.005	0.684±0.011	0.695±0.004	0.709±0.007	0.560±0.011	0.566±0.011	0.561±0.009	0.456±0.013	0.410±0.018	0.428±0.010
	GRAND+	0.927±0.004	0.682±0.011	0.693±0.006	0.715±0.008	0.554±0.008	0.568±0.013	0.557±0.011	0.455±0.012	0.416±0.013	0.428±0.011
	LR-GCL	0.933±0.006	0.699±0.015	0.721±0.011	0.742±0.015	0.575±0.014	0.595±0.018	0.588±0.015	0.469±0.015	0.438±0.015	0.453±0.017
ogbn-arxiv	GCN	0.717±0.003	0.401±0.014	0.421±0.014	0.478±0.010	0.336±0.011	0.346±0.021	0.339±0.012	0.286±0.022	0.256±0.010	0.294±0.013
	S ² GC	0.712±0.003	0.417±0.017	0.429±0.014	0.492±0.010	0.344±0.016	0.353±0.031	0.343±0.009	0.297±0.023	0.266±0.013	0.284±0.012
	GCE	0.720±0.004	0.410±0.018	0.428±0.008	0.480±0.014	0.348±0.019	0.344±0.019	0.342±0.015	0.310±0.014	0.260±0.011	0.275±0.015
	UnionNET	0.724±0.006	0.429±0.021	0.449±0.007	0.485±0.012	0.362±0.018	0.367±0.008	0.340±0.009	0.332±0.019	0.269±0.013	0.280±0.012
	NRGNN	0.721±0.006	0.449±0.014	0.466±0.009	0.485±0.012	0.371±0.020	0.379±0.008	0.342±0.011	0.330±0.018	0.271±0.018	0.300±0.010
	RTGNN	0.718±0.004	0.443±0.012	0.464±0.012	0.484±0.014	0.380±0.011	0.384±0.013	0.340±0.017	0.335±0.011	0.285±0.015	0.301±0.006
	SUGRL	0.693±0.002	0.439±0.010	0.467±0.010	0.480±0.012	0.365±0.013	0.385±0.011	0.341±0.009	0.327±0.011	0.275±0.011	0.295±0.011
	MERIT	0.717±0.004	0.442±0.009	0.463±0.009	0.483±0.010	0.368±0.011	0.381±0.011	0.341±0.012	0.324±0.012	0.272±0.010	0.304±0.009
	ARIEL	0.717±0.004	0.448±0.013	0.471±0.013							

Table 4: Performance comparison for node classification on Wiki-CS, Amazon-Computers, and Amazon-Photos with asymmetric label noise, symmetric label noise, and attribute noise.

Dataset	Methods	Noise Level									
		0	40			60			80		
		-	Asymmetric	Symmetric	Attribute	Asymmetric	Symmetric	Attribute	Asymmetric	Symmetric	Attribute
Wiki-CS	GCN	0.918±0.001	0.645±0.009	0.656±0.006	0.702±0.010	0.511±0.013	0.501±0.009	0.531±0.010	0.429±0.022	0.389±0.011	0.415±0.013
	S ² GC	0.918±0.001	0.657±0.012	0.663±0.006	0.713±0.010	0.516±0.013	0.514±0.009	0.556±0.009	0.437±0.020	0.396±0.010	0.422±0.012
	GCE	0.922±0.003	0.662±0.017	0.659±0.007	0.705±0.014	0.515±0.016	0.502±0.007	0.539±0.009	0.443±0.017	0.389±0.012	0.412±0.011
	UnionNET	0.918±0.002	0.669±0.023	0.671±0.013	0.706±0.012	0.525±0.011	0.529±0.011	0.540±0.012	0.458±0.015	0.401±0.011	0.420±0.007
	NRGNN	0.919±0.002	0.678±0.014	0.689±0.009	0.705±0.012	0.545±0.021	0.556±0.011	0.546±0.011	0.461±0.012	0.410±0.012	0.417±0.007
	RTGNN	0.920±0.005	0.678±0.012	0.691±0.009	0.712±0.008	0.559±0.010	0.569±0.011	0.560±0.008	0.455±0.015	0.415±0.015	0.412±0.014
	SUGRL	0.922±0.005	0.675±0.010	0.695±0.010	0.714±0.006	0.550±0.011	0.560±0.011	0.561±0.007	0.449±0.011	0.411±0.011	0.429±0.008
	MERIT	0.924±0.004	0.679±0.011	0.689±0.008	0.709±0.005	0.552±0.014	0.562±0.014	0.562±0.011	0.452±0.013	0.403±0.013	0.426±0.005
	ARIEL	0.925±0.004	0.682±0.011	0.699±0.009	0.712±0.005	0.555±0.011	0.566±0.011	0.556±0.011	0.454±0.014	0.415±0.019	0.427±0.013
	SFA	0.925±0.009	0.682±0.011	0.690±0.012	0.715±0.012	0.555±0.015	0.567±0.014	0.565±0.013	0.458±0.013	0.402±0.013	0.429±0.015
	Sel-CI	0.922±0.008	0.684±0.009	0.694±0.012	0.714±0.010	0.557±0.013	0.568±0.013	0.566±0.010	0.457±0.013	0.412±0.017	0.425±0.009
	Jo-SRC	0.921±0.005	0.684±0.011	0.695±0.004	0.709±0.007	0.560±0.011	0.566±0.011	0.561±0.009	0.456±0.013	0.410±0.018	0.428±0.010
	GRAND+	0.927±0.004	0.682±0.011	0.693±0.006	0.715±0.008	0.554±0.008	0.568±0.013	0.557±0.011	0.455±0.012	0.416±0.013	0.428±0.011
	LR-GCL	0.933±0.006	0.699±0.015	0.721±0.011	0.742±0.015	0.575±0.014	0.595±0.018	0.588±0.015	0.469±0.015	0.438±0.015	0.453±0.017
Amazon-Computers	GCN	0.815±0.005	0.547±0.015	0.636±0.007	0.639±0.008	0.405±0.014	0.517±0.010	0.439±0.012	0.265±0.012	0.354±0.014	0.317±0.013
	S ² GC	0.835±0.002	0.569±0.007	0.664±0.007	0.661±0.007	0.422±0.010	0.535±0.010	0.454±0.011	0.279±0.014	0.366±0.014	0.320±0.013
	GCE	0.819±0.004	0.573±0.011	0.652±0.008	0.650±0.014	0.449±0.011	0.509±0.011	0.445±0.015	0.280±0.013	0.353±0.013	0.325±0.015
	UnionNET	0.820±0.006	0.569±0.014	0.664±0.007	0.653±0.012	0.452±0.010	0.541±0.010	0.450±0.009	0.283±0.014	0.370±0.011	0.320±0.012
	NRGNN	0.822±0.006	0.571±0.019	0.676±0.007	0.645±0.012	0.470±0.014	0.548±0.014	0.451±0.011	0.282±0.022	0.373±0.012	0.326±0.010
	RTGNN	0.828±0.003	0.570±0.010	0.682±0.008	0.678±0.011	0.474±0.011	0.555±0.010	0.457±0.009	0.280±0.011	0.386±0.014	0.342±0.016
	SUGRL	0.834±0.005	0.564±0.011	0.674±0.012	0.675±0.009	0.468±0.011	0.552±0.011	0.452±0.012	0.280±0.012	0.381±0.012	0.338±0.014
	MERIT	0.831±0.005	0.560±0.008	0.670±0.008	0.671±0.009	0.467±0.013	0.547±0.013	0.450±0.014	0.277±0.013	0.385±0.013	0.335±0.009
	ARIEL	0.843±0.004	0.573±0.013	0.681±0.010	0.675±0.009	0.471±0.012	0.553±0.012	0.455±0.014	0.284±0.014	0.389±0.013	0.343±0.013
	SFA	0.839±0.010	0.564±0.011	0.677±0.013	0.676±0.015	0.473±0.014	0.549±0.014	0.457±0.014	0.282±0.016	0.389±0.013	0.344±0.017
	Sel-CI	0.828±0.002	0.570±0.010	0.685±0.012	0.676±0.009	0.472±0.013	0.554±0.014	0.455±0.011	0.282±0.017	0.389±0.013	0.341±0.015
	Jo-SRC	0.825±0.005	0.571±0.006	0.684±0.013	0.679±0.007	0.473±0.011	0.556±0.008	0.458±0.012	0.285±0.013	0.387±0.018	0.345±0.018
	GRAND+	0.858±0.006	0.570±0.009	0.682±0.007	0.678±0.011	0.472±0.010	0.554±0.008	0.456±0.012	0.284±0.015	0.387±0.015	0.345±0.013
	LR-GCL	0.858±0.006	0.589±0.011	0.713±0.007	0.695±0.011	0.492±0.011	0.587±0.013	0.477±0.012	0.306±0.012	0.419±0.012	0.363±0.011
Amazon-Photos	GCN	0.703±0.005	0.475±0.023	0.501±0.013	0.529±0.009	0.351±0.014	0.341±0.014	0.372±0.011	0.291±0.022	0.281±0.019	0.290±0.014
	S ² GC	0.736±0.005	0.488±0.013	0.528±0.013	0.553±0.008	0.363±0.012	0.367±0.014	0.390±0.013	0.304±0.024	0.284±0.019	0.288±0.011
	GCE	0.705±0.004	0.490±0.016	0.512±0.014	0.540±0.014	0.362±0.015	0.352±0.010	0.381±0.009	0.309±0.012	0.285±0.014	0.285±0.011
	UnionNET	0.706±0.006	0.499±0.015	0.547±0.014	0.545±0.013	0.379±0.013	0.399±0.013	0.379±0.012	0.322±0.021	0.302±0.013	0.290±0.012
	NRGNN	0.710±0.006	0.498±0.015	0.546±0.015	0.538±0.011	0.382±0.016	0.412±0.016	0.377±0.012	0.336±0.021	0.309±0.018	0.284±0.009
	RTGNN	0.746±0.008	0.498±0.007	0.556±0.007	0.550±0.012	0.392±0.010	0.424±0.013	0.390±0.014	0.348±0.017	0.308±0.016	0.302±0.011
	SUGRL	0.730±0.005	0.493±0.011	0.541±0.011	0.544±0.010	0.376±0.009	0.421±0.009	0.388±0.009	0.339±0.010	0.305±0.010	0.300±0.009
	MERIT	0.740±0.007	0.496±0.012	0.536±0.012	0.542±0.010	0.383±0.011	0.425±0.011	0.387±0.008	0.344±0.014	0.301±0.014	0.295±0.009
	SFA	0.740±0.011	0.502±0.014	0.532±0.015	0.547±0.013	0.390±0.014	0.433±0.014	0.389±0.012	0.347±0.016	0.312±0.015	0.299±0.013
	ARIEL	0.727±0.007	0.500±0.008	0.550±0.013	0.548±0.008	0.391±0.009	0.427±0.012	0.389±0.014	0.349±0.014	0.307±0.013	0.299±0.013
	Sel-CI	0.725±0.008	0.499±0.012	0.551±0.010	0.549±0.008	0.389±0.011	0.426±0.008	0.391±0.020	0.350±0.018	0.310±0.015	0.300±0.017
	Jo-SRC	0.730±0.005	0.500±0.013	0.555±0.011	0.551±0.011	0.394±0.013	0.425±0.013	0.393±0.013	0.351±0.013	0.305±0.018	0.303±0.013
	GRAND+	0.756±0.004	0.497±0.010	0.553±0.010	0.552±0.011	0.390±0.013	0.422±0.013	0.387±0.013	0.348±0.013	0.309±0.014	0.302±0.012
	LR-GCL	0.757±0.010	0.520±0.013	0.581±0.013	0.570±0.007	0.410±0.014	0.455±0.014	0.406±0.012	0.369±0.012	0.335±0.014	0.318±0.010

Table 5: Performance comparison for node classification by inductive linear classifier, transductive two-layer GCN classifier, and transductive classifier used in LR-GCL. The comparisons are performed on Cora.

Methods	Noise Level									
	0	40			60			80		
	-	Asymmetric	Symmetric	Attribute	Asymmetric	Symmetric	Attribute	Asymmetric	Symmetric	Attribute
SUGRL (original, inductive classifier)	0.834±0.005	0.564±0.011	0.674±0.012	0.675±0.009	0.468±0.011	0.552±0.011	0.452±0.012	0.280±0.012	0.381±0.012	0.338±0.014
SUGRL + transductive GCN	0.833±0.006	0.562±0.013	0.675±0.015	0.673±0.012	0.470±0.011	0.551±0.011	0.454±0.012	0.280±0.012	0.380±0.012	0.340±0.014
SUGRL + linear transductive classifier	0.836±0.007	0.568±0.013	0.677±0.010	0.674±0.011	0.472±0.011	0.555±0.011	0.457±0.012	0.284±0.012	0.383±0.012	0.341±0.014
MERIT (original, inductive classifier)	0.831±0.005	0.560±0.008	0.670±0.008	0.671±0.009	0.467±0.013	0.547±0.013	0.450±0.014	0.277±0.013	0.385±0.013	0.335±0.009
MERIT + transductive GCN	0.831±0.007	0.562±0.011	0.668±0.013	0.672±0.014	0.466±0.013	0.549±0.015	0.451±0.016	0.276±0.012	0.382±0.014	0.337±0.013
MERIT + linear transductive classifier	0.833±0.003	0.562±0.014	0.673±0.012	0.673±0.011	0.466±0.015	0.546±0.016	0.453±0.017	0.280±0.016	0.386±0.011	0.336±0.014
SFA (original, inductive classifier)	0.839±0.010	0.564±0.011	0.677±0.013	0.676±0.015	0.473±0.014	0.549±0.014	0.457±0.014	0.282±0.016	0.389±0.013	0.344±0.017
SFA + transductive GCN	0.837±0.013	0.565±0.011	0.673±0.017	0.673±0.018	0.474±0.016	0.551±0.015	0.453±0.018	0.277±0.016	0.389±0.015	0.343±0.019
SFA + linear transductive classifier	0.841±0.015	0.566±0.013	0.678±0.014	0.679±0.014	0.477±0.015	0.552±0.012	0.456±0.016	0.284±0.017	0.391±0.015	0.348±0.019
LR-GCL	0.858±0.006	0.589±0.011	0.713±0.007	0.695±0.011	0.492±0.011	0.587±0.013	0.477±0.012	0.306±0.012	0.419±0.012	0.363±0.011

three benchmark datasets. For example, LRA-GCL outperforms the best baseline method by 2.3% in node classification accuracy on PubMed with 80% symmetric label noise.

Table 6: Comparisons in complexity of kernels.

Datasets		MERIT	SFA	Jo-SRC	LR-GCL
Cora	Complex.	0.5485	0.5749	0.5383	0.1675
	h	1455	1532	1431	433 (rank)
Citeseer	Complex.	0.4233	0.4546	0.4090	0.1178
	h	1347	1479	1330	366
PubMed	Complex.	0.9770	0.1095	0.0932	0.0674
	h	1690	1874	1667	1183
Wiki-CS	Complex.	0.1615	0.1762	0.1498	0.1062
	h	1784	1986	1639	1170
Amazon-Computers	Complex.	0.1132	0.1217	0.1110	0.0655
	h	1467	1579	1433	874
Amazon-Photos	Complex.	0.1875	0.2047	0.1823	0.1007
	h	1397	1532	1353	750
Coauthor-CS	Complex.	0.0764	0.0859	0.0749	0.0622
	h	1657	1874	1605	1120
ogbn-arxiv	Complex.	0.0124	0.0139	0.0117	0.0103
	h	1769	1920	1653	1354

5.4 Node Classification Results for GCL Methods with different types of classifiers

Existing GCL methods, such as MERIT, SUGRL, and SFA, first train a graph encoder with graph contrastive learning objectives such as InfoNCE (Jin et al., 2021). After obtaining the node representation learned by contrastive learning, a linear layer for classification is trained in the supervised setting. In contrast, LR-GCL adopts a transductive classifier on top of the node representation obtained by contrastive learning. For fair comparisons with previous GCL methods, we also train the compared GCL baselines with the same transductive classifier as in LR-GCL and a two-layer transductive GCN classifier.

Table 7: Ablation study on the value of rank r_0 in the optimization problem (3) on Cora with different levels of asymmetric and symmetric label noise. The accuracy with the optimal rank is shown in the last row. The accuracy difference against the optimal rank is shown for other ranks.

Rank	Noise Level						
	0	40		60		80	
	-	Asymmetric	Symmetric	Asymmetric	Symmetric	Asymmetric	Symmetric
0.1 $\min\{N, d\}$	-0.002	-0.001	-0.002	-0.002	-0.001	-0.001	-0.000
0.2 $\min\{N, d\}$	-0.000	-0.000	-0.000	-0.000	-0.000	-0.000	-0.000
0.3 $\min\{N, d\}$	-0.000	-0.000	-0.001	-0.002	-0.001	-0.000	-0.001
0.4 $\min\{N, d\}$	-0.001	-0.003	-0.002	-0.001	-0.002	-0.002	-0.002
0.5 $\min\{N, d\}$	-0.001	-0.002	-0.003	-0.003	-0.003	-0.001	-0.002
0.6 $\min\{N, d\}$	-0.003	-0.002	-0.002	-0.003	-0.002	-0.002	-0.003
0.7 $\min\{N, d\}$	-0.003	-0.004	-0.003	-0.004	-0.004	-0.004	-0.005
0.8 $\min\{N, d\}$	-0.002	-0.005	-0.006	-0.006	-0.006	-0.007	-0.007
0.9 $\min\{N, d\}$	-0.004	-0.004	-0.005	-0.007	-0.008	-0.008	-0.006
$\min\{N, d\}$	-0.004	-0.004	-0.007	-0.007	-0.008	-0.010	-0.008
optimal	0.858	0.589	0.713	0.492	0.587	0.306	0.419

5.5 Study in the Kernel Complexity

Given the node representations \mathbf{H} learned by LR-GCL and the competing GCL methods, the kernel com-

plexity of the gram matrix $\mathbf{K} = \frac{1}{n}\mathbf{H}\mathbf{H}^\top$ can be computed by $\min_{h \in [0, n]} \left(\frac{h}{n} + \sqrt{\frac{\sum_{i=h+1}^n \hat{\lambda}_i}{n}} \right)$.

In this section, we compute such kernel complexity for the gram matrix of node representations learned by LR-GCL and the competing GCL methods on different datasets with attribute noise of level 40. The

results are shown in Table 6. It is observed that the gram matrix of the node representations learned by LR-GCL exhibits much lower complexity, which suggests that the transductive classifiers trained on the node representations learned by LR-GCL have lower generalization errors on the unlabeled nodes.

5.6 Ablation Study on the Rank in the Truncated Nuclear Norm

We perform ablation study on the value of rank r_0 in the truncated nuclear norm $\|\mathbf{H}\|_{r_0}$ in the loss function (2) of LR-GCL. It is observed from Table 7 that the performance of our LR-GCL is consistently close to the best performance among all the choices of the rank when r_0 is between $0.1 \min\{N, d\}$ and $0.3 \min\{N, d\}$.

Table 8: Training time (seconds) comparisons for node classification.

Methods	Cora	Citeseer	PubMed	Coauthor-CS	Wiki-CS	Computer	Photo	ogbn-arxiv
GCN	11.5	13.7	38.6	43.2	22.3	30.2	19.0	215.1
S ² GC	20.7	22.5	47.2	57.2	27.6	38.5	22.2	243.7
GCE	32.6	36.9	67.3	80.8	37.6	50.1	32.2	346.1
UnionNET	67.5	69.7	100.5	124.2	53.2	69.2	45.3	479.3
NRGNN	72.4	80.5	142.7	189.4	74.3	97.2	62.4	650.2
RTGNN	143.3	169.5	299.5	353.5	153.7	201.5	124.2	1322.2
SUGRL	100.3	122.1	207.4	227.1	107.7	142.8	87.7	946.8
MERIT	167.2	179.2	336.7	375.3	172.3	226.5	140.6	1495.1
ARIEL	156.9	164.3	284.3	332.6	145.1	190.4	118.3	1261.4
SFA	237.5	269.4	457.1	492.3	233.5	304.5	187.2	2013.1
Sel-Cl	177.3	189.9	313.5	352.5	161.7	211.1	130.9	1401.1
Jo-SRC	148.2	157.1	281.0	306.1	144.5	188.0	118.5	1256.0
GRAND+	57.4	68.4	101.7	124.2	54.8	73.8	44.5	479.2
LR-GCL	159.9	174.5	350.7	380.9	180.3	235.7	145.5	1552.7

Furthermore, we compare the training time of LR-GCL with competing baselines in Table 8 in Section B.1 of the appendix.

6 Conclusions

In this paper, we propose a novel GCL encoder termed Low-Rank Graph Contrastive Learning (LR-GCL). LR-GCL is a robust GCL encoder which produces low-rank features inspired by the low frequency property of universal graph datasets and the sharp generalization bound for transductive learning. LR-GCL is trained with prototypical GCL with the truncated nuclear norm as the regularization term. We evaluate the performance of LR-GCL with comparison to competing baselines on semi-supervised or transductive node classification, where graph data are corrupted with noise in either the labels for the node attributes. Extensive experimental results demonstrate that LR-GCL generates more robust node representations with better performance than the current state-of-the-art node representation learning methods.

References

- Kelsey Allen, Evan Shelhamer, Hanul Shin, and Joshua Tenenbaum. Infinite mixture prototypes for few-shot learning. In *International Conference on Machine Learning*, pp. 232–241. PMLR, 2019.
- Sercan Ö Arik and Tomas Pfister. Protoattend: Attention-based prototypical learning. *The Journal of Machine Learning Research*, 21(1):8691–8725, 2020.
- Joan Bruna, Wojciech Zaremba, Arthur Szlam, and Yann LeCun. Spectral networks and locally connected networks on graphs. *ICLR*, 2014.
- Enyan Dai, Charu Aggarwal, and Suhang Wang. Nrgnn: Learning a label noise-resistant graph neural network on sparsely and noisily labeled graphs. *SIGKDD*, 2021.

- Enyan Dai, Wei Jin, Hui Liu, and Suhang Wang. Towards robust graph neural networks for noisy graphs with sparse labels. In *Proceedings of the Fifteenth ACM International Conference on Web Search and Data Mining*, pp. 181–191, 2022.
- Kaize Ding, Zhe Xu, Hanghang Tong, and Huan Liu. Data augmentation for deep graph learning: A survey. *arXiv preprint arXiv:2202.08235*, 2022.
- Shengyu Feng, Baoyu Jing, Yada Zhu, and Hanghang Tong. Adversarial graph contrastive learning with information regularization. In *Proceedings of the ACM Web Conference 2022*, pp. 1362–1371, 2022a.
- Wenzheng Feng, Yuxiao Dong, Tinglin Huang, Ziqi Yin, Xu Cheng, Evgeny Kharlamov, and Jie Tang. Grand+: Scalable graph random neural networks. In *Proceedings of the ACM Web Conference 2022*, pp. 3248–3258, 2022b.
- Jacob Goldberger and Ehud Ben-Reuven. Training deep neural-networks using a noise adaptation layer. 2016.
- Yuanfan Guo, Minghao Xu, Jiawen Li, Bingbing Ni, Xuanyu Zhu, Zhenbang Sun, and Yi Xu. Hcsc: hierarchical contrastive selective coding. In *Proceedings of the IEEE/CVF Conference on Computer Vision and Pattern Recognition*, pp. 9706–9715, 2022.
- Will Hamilton, Zhitao Ying, and Jure Leskovec. Inductive representation learning on large graphs. *NeurIPS*, 30, 2017.
- Bo Han, Quanming Yao, Xingrui Yu, Gang Niu, Miao Xu, Weihua Hu, Ivor Tsang, and Masashi Sugiyama. Co-teaching: Robust training of deep neural networks with extremely noisy labels. pp. 8536–8546, 2018.
- Bo Han, Quanming Yao, Tongliang Liu, Gang Niu, Ivor W Tsang, James T Kwok, and Masashi Sugiyama. A survey of label-noise representation learning: Past, present and future. *arXiv preprint arXiv:2011.04406*, 2020.
- Weihua Hu, Bowen Liu, Joseph Gomes, Marinka Zitnik, Percy Liang, Vijay Pande, and Jure Leskovec. Strategies for pre-training graph neural networks. *arXiv preprint arXiv:1905.12265*, 2019.
- Weihua Hu, Matthias Fey, Marinka Zitnik, Yuxiao Dong, Hongyu Ren, Bowen Liu, Michele Catasta, and Jure Leskovec. Open graph benchmark: Datasets for machine learning on graphs. In *NeurIPS*, 2020.
- Lu Jiang, Zhengyuan Zhou, Thomas Leung, Li-Jia Li, and Li Fei-Fei. Mentornet: Learning data-driven curriculum for very deep neural networks on corrupted labels. In *International Conference on Machine Learning*, pp. 2304–2313. PMLR, 2018.
- Yizhu Jiao, Yun Xiong, Jiawei Zhang, Yao Zhang, Tianqi Zhang, and Yangyong Zhu. Sub-graph contrast for scalable self-supervised graph representation learning. In *2020 IEEE international conference on data mining (ICDM)*, pp. 222–231. IEEE, 2020.
- Ming Jin, Yizhen Zheng, Yuan-Fang Li, Chen Gong, Chuan Zhou, and Shirui Pan. Multi-scale contrastive siamese networks for self-supervised graph representation learning. In *The 30th International Joint Conference on Artificial Intelligence (IJCAI)*, 2021.
- Thomas N. Kipf and Max Welling. Semi-supervised classification with graph convolutional networks. In *ICLR*, 2017.
- Vignesh Kothapalli, Tom Tirer, and Joan Bruna. A neural collapse perspective on feature evolution in graph neural networks. In Alice Oh, Tristan Naumann, Amir Globerson, Kate Saenko, Moritz Hardt, and Sergey Levine (eds.), *Advances in Neural Information Processing Systems 36: Annual Conference on Neural Information Processing Systems 2023, NeurIPS 2023, New Orleans, LA, USA, December 10 - 16, 2023*, 2023.
- Namkyeong Lee, Junseok Lee, and Chanyoung Park. Augmentation-free self-supervised learning on graphs. In *Proceedings of the AAAI Conference on Artificial Intelligence*, volume 36, pp. 7372–7380, 2022.

- Junnan Li, Richard Socher, and Steven CH Hoi. Dividemix: Learning with noisy labels as semi-supervised learning. *arXiv preprint arXiv:2002.07394*, 2020.
- Junnan Li, Pan Zhou, Caiming Xiong, and Steven C.H. Hoi. Prototypical contrastive learning of unsupervised representations. In *ICLR*, 2021.
- Shikun Li, Xiaobo Xia, Shiming Ge, and Tongliang Liu. Selective-supervised contrastive learning with noisy labels. In *Proceedings of the IEEE/CVF Conference on Computer Vision and Pattern Recognition*, pp. 316–325, 2022.
- Lu Lin, Jinghui Chen, and Hongning Wang. Spectral augmentation for self-supervised learning on graphs. *ICLR*, 2023.
- Eran Malach and Shai Shalev-Shwartz. Decoupling “when to update” from “how to update”. In *NeurIPS*, pp. 960–970, 2017.
- Péter Mernyei and Cătălina Cangea. Wiki-cs: A wikipedia-based benchmark for graph neural networks. *arXiv preprint arXiv:2007.02901*, 2020.
- Yujie Mo, Liang Peng, Jie Xu, Xiaoshuang Shi, and Xiaofeng Zhu. Simple unsupervised graph representation learning. *AAAI*, 2022.
- Hoang NT, Choong Jin, and Tsuyoshi Murata. Learning graph neural networks with noisy labels. In *2nd ICLR Learning from Limited Labeled Data (LLD) Workshop*, 2019.
- Giorgio Patrini, Alessandro Rozza, Aditya Krishna Menon, Richard Nock, and Lizhen Qu. Making deep neural networks robust to label noise: A loss correction approach. In *CVPR*, pp. 1944–1952, 2017.
- Zhen Peng, Wenbing Huang, Minnan Luo, Qinghua Zheng, Yu Rong, Tingyang Xu, and Junzhou Huang. Graph representation learning via graphical mutual information maximization. In *Proceedings of The Web Conference 2020*, pp. 259–270, 2020.
- Siyi Qian, Haochao Ying, Renjun Hu, Jingbo Zhou, Jintai Chen, Danny Z Chen, and Jian Wu. Robust training of graph neural networks via noise governance. *WSDM*, 2022.
- Prithviraj Sen, Galileo Namata, Mustafa Bilgic, Lise Getoor, Brian Galligher, and Tina Eliassi-Rad. Collective classification in network data. *AI Magazine*, 29(3):93–93, 2008.
- Oleksandr Shchur, Maximilian Mumme, Aleksandar Bojchevski, and Stephan Günnemann. Pitfalls of graph neural network evaluation. *arXiv preprint arXiv:1811.05868*, 2018.
- Jake Snell, Kevin Swersky, and Richard Zemel. Prototypical networks for few-shot learning. *Advances in neural information processing systems*, 30, 2017.
- Fan-Yun Sun, Jordan Hoffman, Vikas Verma, and Jian Tang. Infograph: Unsupervised and semi-supervised graph-level representation learning via mutual information maximization. In *ICLR*, 2019.
- Susheel Suresh, Pan Li, Cong Hao, and Jennifer Neville. Adversarial graph augmentation to improve graph contrastive learning. *Advances in Neural Information Processing Systems*, 34:15920–15933, 2021.
- Shantanu Thakoor, Corentin Tallec, Mohammad Gheshlaghi Azar, Rémi Munos, Petar Veličković, and Michal Valko. Bootstrapped representation learning on graphs. In *ICLR 2021 Workshop on Geometrical and Topological Representation Learning*, 2021.
- Ilya O. Tolstikhin, Gilles Blanchard, and Marius Kloft. Localized complexities for transductive learning. In Maria-Florina Balcan, Vitaly Feldman, and Csaba Szepesvári (eds.), *Conference on Learning Theory*, volume 35 of *JMLR Workshop and Conference Proceedings*, pp. 857–884. JMLR.org, 2014.
- Petar Veličković, Guillem Cucurull, Arantxa Casanova, Adriana Romero, Pietro Lio, and Yoshua Bengio. Graph attention networks. *arXiv preprint arXiv:1710.10903*, 2017.

- Petar Veličković, William Fedus, William L. Hamilton, Pietro Liò, Yoshua Bengio, and R Devon Hjelm. Deep graph infomax. In *ICLR*, 2019.
- Haonan Wang, Jieyu Zhang, Qi Zhu, and Wei Huang. Augmentation-free graph contrastive learning with performance guarantee. *arXiv preprint arXiv:2204.04874*, 2022.
- Keyulu Xu, Weihua Hu, Jure Leskovec, and Stefanie Jegelka. How powerful are graph neural networks? *ICLR*, 2019.
- Minghao Xu, Hang Wang, Bingbing Ni, Hongyu Guo, and Jian Tang. Self-supervised graph-level representation learning with local and global structure. In *International Conference on Machine Learning*, pp. 11548–11558. PMLR, 2021.
- Wenjia Xu, Yongqin Xian, Jiuniu Wang, Bernt Schiele, and Zeynep Akata. Attribute prototype network for zero-shot learning. *Advances in Neural Information Processing Systems*, 33:21969–21980, 2020.
- Yingzhen Yang. Sharp generalization of transductive learning: A transductive local rademacher complexity approach. 2023. URL <https://arxiv.org/pdf/2309.16858v1.pdf>.
- Yazhou Yao, Zeren Sun, Chuanyi Zhang, Fumin Shen, Qi Wu, Jian Zhang, and Zhenmin Tang. Jo-src: A contrastive approach for combating noisy labels. In *Proceedings of the IEEE/CVF Conference on Computer Vision and Pattern Recognition*, pp. 5192–5201, 2021.
- Yuning You, Tianlong Chen, Yongduo Sui, Ting Chen, Zhangyang Wang, and Yang Shen. Graph contrastive learning with augmentations. *Advances in Neural Information Processing Systems*, 33:5812–5823, 2020.
- Yuning You, Tianlong Chen, Yang Shen, and Zhangyang Wang. Graph contrastive learning automated. In *International Conference on Machine Learning*, pp. 12121–12132. PMLR, 2021.
- Xingrui Yu, Bo Han, Jiangchao Yao, Gang Niu, Ivor W Tsang, and Masashi Sugiyama. How does disagreement help generalization against label corruption? 2019.
- Chiyuan Zhang, Samy Bengio, Moritz Hardt, Benjamin Recht, and Oriol Vinyals. Understanding deep learning (still) requires rethinking generalization. *Communications of the ACM*, 64(3):107–115, 2021.
- Yifei Zhang, Hao Zhu, Zixing Song, Piotr Koniusz, and Irwin King. Spectral feature augmentation for graph contrastive learning and beyond. In *Proceedings of the AAAI Conference on Artificial Intelligence*, volume 37, pp. 11289–11297, 2023.
- Zhilu Zhang and Mert Sabuncu. Generalized cross entropy loss for training deep neural networks with noisy labels. *Advances in neural information processing systems*, 31, 2018.
- Hao Zhu and Piotr Koniusz. Simple spectral graph convolution. In *International Conference on Learning Representations*, 2020.
- Jun Zhuang and Mohammad Al Hasan. Defending graph convolutional networks against dynamic graph perturbations via bayesian self-supervision. In *Proceedings of the AAAI Conference on Artificial Intelligence*, volume 36, pp. 4405–4413, 2022.

A Theoretical Results

We present the proof of Theorem 4.1 in this section.

Proof of Theorem 4.1. It can be verified that at the t -th iteration of gradient descent for $t \geq 1$, we have

$$\mathbf{W}^{(t)} = \mathbf{W}^{(t-1)} - \eta [\mathbf{H}]_{\mathcal{L}}^{\top} [\mathbf{H}\mathbf{W}^{(t-1)} - \mathbf{Y}]_{\mathcal{L}}. \quad (5)$$

It follows by (5) that

$$[\mathbf{H}]_{\mathcal{L}} \mathbf{W}^{(t)} = [\mathbf{H}]_{\mathcal{L}} \mathbf{W}^{(t-1)} - \eta [\mathbf{K}]_{\mathcal{L}, \mathcal{L}} \left(\mathbf{H} \mathbf{W}^{(t-1)} - \mathbf{Y} \right), \quad (6)$$

where $\mathbf{K}_{\mathcal{L}, \mathcal{L}} := [\mathbf{H}]_{\mathcal{L}} [\mathbf{H}]_{\mathcal{L}}^{\top} \in \mathbb{R}^{m \times m}$. With $\mathbf{F}(\mathbf{W}, t) = \mathbf{H} \mathbf{W}^{(t)}$, it follows by (6) that

$$[\mathbf{F}(\mathbf{W}, t) - \mathbf{Y}]_{\mathcal{L}} = \left(\mathbf{I}_m - \eta [\mathbf{K}]_{\mathcal{L}, \mathcal{L}} \right) [\mathbf{F}(\mathbf{W}, t-1) - \mathbf{Y}]_{\mathcal{L}}.$$

It follows from the above equality that

$$[\mathbf{F}(\mathbf{W}, t) - \mathbf{Y}]_{\mathcal{L}} = \left(\mathbf{I}_m - \eta [\mathbf{K}]_{\mathcal{L}, \mathcal{L}} \right)^t [\mathbf{F}(\mathbf{W}, t-1) - \mathbf{Y}]_{\mathcal{L}} = - \left(\mathbf{I}_m - \eta [\mathbf{K}]_{\mathcal{L}, \mathcal{L}} \right)^t [\mathbf{Y}]_{\mathcal{L}},$$

so that

$$\|[\mathbf{F}(\mathbf{W}, t) - \mathbf{Y}]_{\mathcal{L}}\|_{\mathbf{F}} \leq \left\| \left(\mathbf{I}_m - \eta [\mathbf{K}]_{\mathcal{L}, \mathcal{L}} \right)^t [\mathbf{Y}]_{\mathcal{L}} \right\|_{\mathbf{F}}. \quad (7)$$

We apply (Yang, 2023, Corollary 3.7) to obtain the following bound for the test loss $\frac{1}{u} \|[\mathbf{F}(\mathbf{W}, t) - \mathbf{Y}]_{\mathcal{U}}\|_{\mathbf{F}}^2$:

$$\frac{1}{u} \|[\mathbf{F}(\mathbf{W}, t) - \mathbf{Y}]_{\mathcal{U}}\|_{\mathbf{F}}^2 \leq \frac{c_0}{m} \|[\mathbf{F}(\mathbf{W}, t) - \mathbf{Y}]_{\mathcal{L}}\|_{\mathbf{F}}^2 + c_1 \min_{0 \leq Q \leq n} r(u, m, Q) + \frac{c_2 x}{u}, \quad (8)$$

with

$$r(u, m, Q) := Q \left(\frac{1}{u} + \frac{1}{m} \right) + \left(\sqrt{\frac{\sum_{q=Q+1}^N \hat{\lambda}_q^2}{u}} + \sqrt{\frac{\sum_{q=Q+1}^N \hat{\lambda}_q^2}{m}} \right),$$

where c_0, c_1, c_2 are positive numbers depending on \mathbf{U} , $\{\hat{\lambda}_i\}_{i=1}^r$, and τ_0 with $\tau_0^2 = \max_{i \in [N]} \mathbf{K}_{ii}$.

It follows by (7) and (8) with $Q = r_0$ that

$$\begin{aligned} & \frac{1}{u} \|[\mathbf{F}(\mathbf{W}, t) - \mathbf{Y}]_{\mathcal{U}}\|_{\mathbf{F}}^2 \\ & \leq \frac{c_0}{m} \left\| \left(\mathbf{I}_m - \eta [\mathbf{K}]_{\mathcal{L}, \mathcal{L}} \right)^t [\mathbf{Y}]_{\mathcal{L}} \right\|_{\mathbf{F}}^2 + c_1 r_0 \left(\frac{1}{u} + \frac{1}{m} \right) + \left(\sqrt{\frac{\sum_{q=r_0+1}^N \hat{\lambda}_q^2}{u}} + \sqrt{\frac{\sum_{q=r_0+1}^N \hat{\lambda}_q^2}{m}} \right) + \frac{c_2 x}{u}, \end{aligned} \quad (9)$$

which completes the proof with $\sqrt{\sum_{q=r_0+1}^N \hat{\lambda}_q^2} \leq \|\mathbf{H}\|_{r_0}$. □

B Training Time Comparison and Eigen-Projection and Concentration Entropy Analysis for More Datasets

B.1 Training Time Comparison

In this section, we compare the training time of LR-GCL against other baseline methods on all benchmark datasets. The training time of LR-GCL includes the training time of robust graph contrastive learning, the time of the SVD computation of the kernel, and the training time of the transductive classifier. For the competing GCL methods, we include both the training time of the GCL encoder and the downstream classifier. The training time is evaluated on one 80 GB A100 GPU. The results are shown in Table 8. It is observed that the LR-GCL takes similar training time as the competing GCL methods, such as SFA and MERIT.

C Eigen-Projection and Concentration Entropy Analysis on Additional Datasets

Figure 3 illustrates the eigen-projection and energy concentration ratio for Coauthor-CS, Amazon-Computers, Amazon-Photos, and ogbn-arxiv.

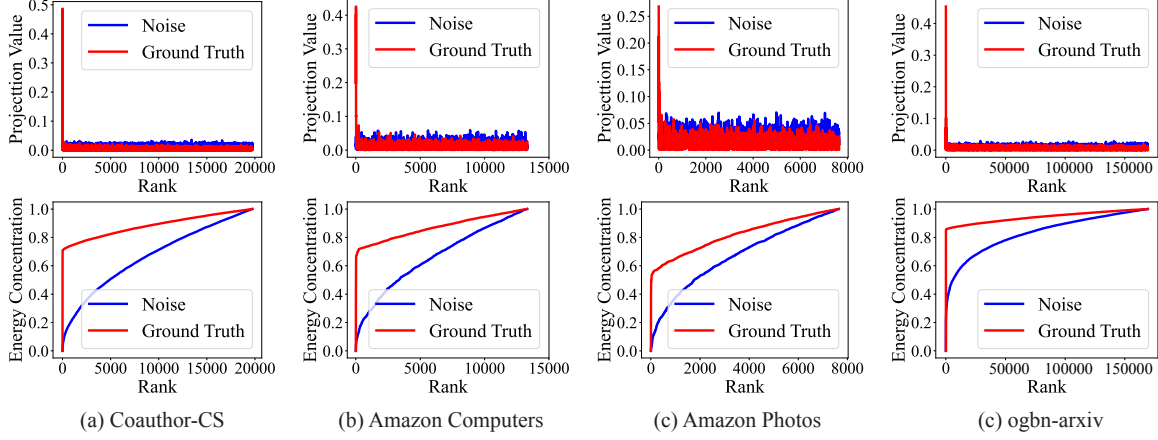


Figure 3: Eigen-projection (first row) and energy concentration (second row) on Coauthor-CS, Amazon-Computers, Amazon-Photos, and ogbn-arxiv. By the rank of $0.2 \min \{N, d\}$, the concentration entropy on Coauthor-CS, Amazon-Computers, Amazon-Photos, and ogbn-arxiv are 0.779, 0.809, 0.752, and 0.787.